Rerefinement of the crystal structure of $SnTe_{0.73(2)}Se_{0.27(2)}$ from single-crystal X-ray diffraction data

Silvana Moris[a] and Antonio Galdámez[b]*

[a]Centro de Investigación de Estudios Avanzados del Maule (CIEAM), Vicerrectoría de Investigación y Postgrado, Universidad Católica del Maule, Avenida San Miguel 3605, Talca 3480112, Chile, and [b]Universidad de Chile, Facultad de Ciencias, Departamento de Química, Casilla 653, Santiago, Chile. *Correspondence e-mail: agaldamez@uchile.cl

Compounds of the solid solution series $SnTe_{1-x}Se_x$, derived from pristine SnSe and SnTe, are considered as thermoelectric lead-free materials. The crystal structure re-refinement of NaCl-type $SnTe_{0.73(2)}Se_{0.27(2)}$ is based on single-crystal X-ray diffraction data and results in higher precision of the bond length [Sn—(Te,Se) = 3.0798 (3) Å] compared to a previous report on basis of powder X-ray data [Krebs & Langner (1964). *Z. Anorg. Allg. Chem.* **334**, 37–49].

3D view
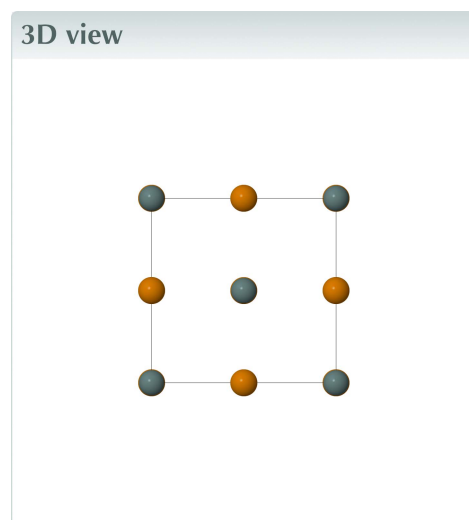
Structure description

Lead chalcogenides have proven to exhibit an excellent performance as thermoelectric materials. However, due to the current environmental regulations, generating lead-free materials with thermoelectric properties becomes necessary. In this regard, semi-conductors of the solid-solution series $SnTe_{1-x}Se_x$ have the potential to be good lead-free thermoelectric materials at mid/high temperatures (Banik & Biswas, 2014). Characterization of phases in the $SnTe_{1-x}Se_x$ system on the basis of powder X-ray diffraction data has been reported previously (Krebs & Langner, 1964; Totani *et al.*, 1968; Liu & Chang, 1992; Ariponnammacl *et al.*, 1996; Majid & Legendre, 1998; Banik & Biswas, 2014). The powder patterns were indexed in the cubic crystal system, revealing an NaCl-type crystal structure. The reported unit-cell parameters (Liu & Chang, 1992) of $SnTe_{0.9}Se_{0.1}$ and $SnTe_{0.75}Se_{0.25}$ are a = 6.2433 Å and a = 6.2188 Å, respectively. The $SnTe_{1-x}Se_x$ (x = 0 to 0.15) samples could be viewed as solid solutions that obey Vegard's law (Banik & Biswas, 2014). The parameter a of the cubic unit cell increases from approximately 6.23 to 6.27 Å with decreasing Se content x, as determined from the powder pattern.

Here, we report the crystal structure rerefinement of the solid solution with composition $SnTe_{0.73(2)}Se_{0.27(2)}$ from single-crystal X-ray diffraction data. The crystal structure of $SnTe_{0.73(2)}Se_{0.27(2)}$ likewise adopts the NaCl type (Fig. 1) with an intermediate value of a [6.1595 (5) Å] between those of the binary compounds SnTe (6.314 Å) and SnSe (5.99 Å), which is attributed to the different radii of Te and Se. The cell parameter reported by Liu & Chang (1992) of a = 6.2188 Å for $SnTe_{0.75}Se_{0.25}$ at room temperature is somewhat higher than that of $SnTe_{0.73(2)}Se_{0.27(2)}$ determined at 150 K. The present study allowed for a higher precision with respect to the bond lengths in $SnTe_{0.73(2)}Se_{0.27(2)}$, which is Sn—(Te,Se) = 3.0798 (3) Å.

Synthesis and crystallization

Single crystals of the title compound were obtained seren-dipitously by application of the high-temperature ceramic method. Powders of silver (99.99%), tin (99.99%), bismuth (99.999%), selenium (99%) and tellurium (99%) were weighted in an molar ratio of 1:2:1:2.5:2.5. All manipulations were carried out under an argon atmosphere. The reaction mixture was sealed in an evacuated silica ampoule and placed in a programmable furnace (Figueroa-Millon et al., 2018). The ampoule was slowly heated from room temperature to 1023 K at a rate of 333 K min^{-1} to the maximum temperature and held for 7 d, followed by slow cooling to room temperature at a rate of 278 K h^{-1}. The reaction product consisted of a gray metallic powder (yield ~99%) accompanied by black octahedrally shaped single crystals (yield ~1%) that were manually separated for the X-ray diffraction study. The refined composition of the measured crystal is $SnTe_{0.73(2)}Se_{0.27(2)}$.

Figure 1
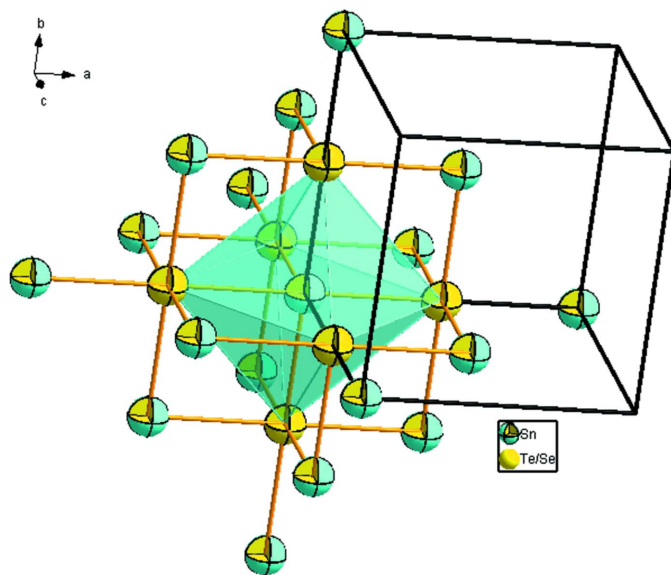A view of the NaCl-type crystal structure of $SnTe_{0.73(2)}Se_{0.27(2)}$. Displacement ellipsoids are drawn at the 50% probability level.

Table 1
Experimental details.

Crystal data	
Chemical formula	$SnTe_{0.73}Se_{0.27}$
M_r	233.28
Crystal system, space group	Cubic, $Fm\bar{3}m$
Temperature (K)	150
a (Å)	6.1595 (5)
V (Å^3)	233.69 (6)
Z	4
Radiation type	Mo $K\alpha$
μ (mm^{-1})	23.61
Crystal size (mm)	$0.10 \times 0.08 \times 0.07$
Data collection	
Diffractometer	Nonius KappaCCD
Absorption correction	Multi-scan (SADABS; Krause et al., 2015)
T_{min}, T_{max}	0.103, 0.205
No. of measured, independent and observed [$I > 2\sigma(I)$] reflections	396, 33, 33
R_{int}	0.042
$(\sin\theta/\lambda)_{max}$ (Å^{-1})	0.703
Refinement	
$R[F^2 > 2\sigma(F^2)]$, $wR(F^2)$, S	0.045, 0.115, 1.49
No. of reflections	33
No. of parameters	4
$\Delta\rho_{max}$, $\Delta\rho_{min}$ (e Å^{-3})	1.92, −1.84

Computer programs: COLLECT (Bruker, 1997-2004), DIRAX/LSQ (Duisenberg et al., 2003), EVALCCD (Duisenberg et al., 2003), olex2.solve (Bourhis et al., 2015), SHELXL (Sheldrick, 2015), OLEX2 (Dolomanov et al., 2009) and publCIF (Westrip, 2010).

Refinement

Crystal data, data collection, and structure refinement details are summarized in Table 1. For the shared chalcogenide site, the sum of site occupation factors (SOF) was constrained to 1, and the anisotropic displacement parameters were constrained to be the same. The crystal under investigation consisted of two domains with approximately equal contribution to the intensity data. The integration procedure showed that the reflections of each domain were clearly separated. For the final intensity data only one domain was used.

References

Ariponnammal, S., Venkateswaran, C. & Natarajan, S. (1996). *Phys. Status Solidi B*, **197**, K1–K4.
Banik, A. & Biswas, K. (2014). *J. Mater. Chem. A*, **2**, 9620–9625.
Bourhis, L. J., Dolomanov, O. V., Gildea, R. J., Howard, J. A. K. & Puschmann, H. (2015). *Acta Cryst.* A**71**, 59–75.
Bruker (1997–2004). *COLLECT*. Bruker AXS Inc., Madison, Wisconsin, USA.
Dolomanov, O. V., Bourhis, L. J., Gildea, R. J., Howard, J. A. K. & Puschmann, H. (2009). *J. Appl. Cryst.* **42**, 339–341.

Duisenberg, A. J. M., Kroon-Batenburg, L. M. J. & Schreurs, A. M. M. (2003). *J. Appl. Cryst.* **36**, 220–229.

Figueroa-Millon, S., Álvarez-Serrano, I., Bérardan, D. & Galdámez, A. (2018). *Mater. Chem. Phys.* **211**, 321–328.

Krause, L., Herbst-Irmer, R., Sheldrick, G. M. & Stalke, D. (2015). *J. Appl. Cryst.* **48**, 3–10.

Krebs, V. & Langner, D. (1964). *Z. Anorg. Allg. Chem.* **334**, 37–49.

Liu, H. & Chang, L. (1992). *J. Alloys Compd.* **185**, 183–190.

Majid, M. & Legendre, B. (1998). *J. Therm. Anal.* **54**, 963–990.

Sheldrick, G. M. (2015). *Acta Cryst.* C**71**, 3–8.

Totani, A., Okazaki, H. & Nakajima, S. (1968). *Trans. Metall. Soc. AIME*, **2426**, 709.

Westrip, S. P. (2010). *J. Appl. Cryst.* **43**, 920–925.

full crystallographic data

Rerefinement of the crystal structure of SnTe$_{0.73(2)}$Se$_{0.27(2)}$ from single-crystal X-ray diffraction data

Silvana Moris and Antonio Galdámez

Tin tellurium selenide

Crystal data

SnTe$_{0.73}$Se$_{0.27}$
$M_r = 233.28$
Cubic, $Fm\overline{3}m$
$a = 6.1595\ (5)$ Å
$V = 233.69\ (6)$ Å^3
$Z = 4$
$F(000) = 389$
$D_x = 6.631$ Mg m^{-3}

Mo $K\alpha$ radiation, $\lambda = 0.71073$ Å
Cell parameters from 553 reflections
$\theta = 5.7–39.8°$
$\mu = 23.61$ mm^{-1}
$T = 150$ K
Octahedron, black
$0.10 \times 0.08 \times 0.07$ mm

Data collection

Nonius KappaCCD
   diffractometer
Radiation source: Enraf Nonius FR590
Graphite monochromator
Detector resolution: 9 pixels mm^{-1}
CCD rotation images, thin slices scans
Absorption correction: multi-scan
   (*SADABS*; Krause *et al.*, 2015)
$T_{min} = 0.103$, $T_{max} = 0.205$

396 measured reflections
33 independent reflections
33 reflections with $I > 2\sigma(I)$
$R_{int} = 0.042$
$\theta_{max} = 30.0°$, $\theta_{min} = 5.7°$
$h = -8 \rightarrow 8$
$k = -7 \rightarrow 8$
$l = -6 \rightarrow 8$

Refinement

Refinement on F^2
Least-squares matrix: full
$R[F^2 > 2\sigma(F^2)] = 0.045$
$wR(F^2) = 0.115$
$S = 1.49$
33 reflections
4 parameters

0 restraints
$w = 1/[\sigma^2(F_o^2) + (0.0583P)^2 + 1.8772P]$
   where $P = (F_o^2 + 2F_c^2)/3$
$(\Delta/\sigma)_{max} < 0.001$
$\Delta\rho_{max} = 1.92$ e Å^{-3}
$\Delta\rho_{min} = -1.84$ e Å^{-3}

Special details

Geometry. All esds (except the esd in the dihedral angle between two l.s. planes) are estimated using the full covariance matrix. The cell esds are taken into account individually in the estimation of esds in distances, angles and torsion angles; correlations between esds in cell parameters are only used when they are defined by crystal symmetry. An approximate (isotropic) treatment of cell esds is used for estimating esds involving l.s. planes.

Fractional atomic coordinates and isotropic or equivalent isotropic displacement parameters (Å²)

	x	y	z	$U_{iso}*/U_{eq}$	Occ. (<1)
Sn	0.000000	0.000000	0.000000	0.0199 (10)	
Te	0.000000	0.000000	0.500000	0.0330 (12)	0.73 (2)
Se	0.000000	0.000000	0.500000	0.0330 (12)	0.27 (2)

Atomic displacement parameters (Å²)

	U^{11}	U^{22}	U^{33}	U^{12}	U^{13}	U^{23}
Sn	0.0199 (10)	0.0199 (10)	0.0199 (10)	0.000	0.000	0.000
Te	0.0330 (12)	0.0330 (12)	0.0330 (12)	0.000	0.000	0.000
Se	0.0330 (12)	0.0330 (12)	0.0330 (12)	0.000	0.000	0.000

Geometric parameters (Å, °)

Sn—Te^i	3.0798 (3)	Sn—Te^{iii}	3.0798 (3)
Sn—Te	3.0798 (3)	Sn—Te^{iv}	3.0798 (3)
Sn—Te^{ii}	3.0798 (3)	Sn—Te^v	3.0798 (3)
Te^i—Sn—Te	90.0	Sn^{vi}—Te—Sn	90.0
Te^i—Sn—Te^{ii}	90.0	Sn^{vi}—Te—Sn^{vii}	90.0
Te—Sn—Te^{ii}	180.0	Sn—Te—Sn^{vii}	180.0
Te^i—Sn—Te^{iii}	90.0	Sn^{vi}—Te—Sn^{viii}	90.0
Te—Sn—Te^{iii}	90.0	Sn—Te—Sn^{viii}	90.0
Te^{ii}—Sn—Te^{iii}	90.0	Sn^{vii}—Te—Sn^{viii}	90.0
Te^i—Sn—Te^{iv}	90.0	Sn^{vi}—Te—Sn^{ix}	90.0
Te—Sn—Te^{iv}	90.0	Sn—Te—Sn^{ix}	90.0
Te^{ii}—Sn—Te^{iv}	90.0	Sn^{vii}—Te—Sn^{ix}	90.0
Te^{iii}—Sn—Te^{iv}	180.0	Sn^{viii}—Te—Sn^{ix}	180.0
Te^i—Sn—Te^v	180.0	Sn^{vi}—Te—Sn^x	180.0
Te—Sn—Te^v	90.0	Sn—Te—Sn^x	90.0
Te^{ii}—Sn—Te^v	90.0	Sn^{vii}—Te—Sn^x	90.0
Te^{iii}—Sn—Te^v	90.0	Sn^{viii}—Te—Sn^x	90.0
Te^{iv}—Sn—Te^v	90.0	Sn^{ix}—Te—Sn^x	90.0

Symmetry codes: (i) $x+1/2, y, z-1/2$; (ii) $x, y, z-1$; (iii) $x, y-1/2, z-1/2$; (iv) $x, y+1/2, z-1/2$; (v) $x-1/2, y, z-1/2$; (vi) $x+1/2, y, z+1/2$; (vii) $x, y, z+1$; (viii) $x, y-1/2, z+1/2$; (ix) $x, y+1/2, z+1/2$; (x) $x-1/2, y, z+1/2$.